

# A CT-study of the Cranial Suture Morphology and its Reorganization during the Obliteration

Silviya Nikolova<sup>1\*</sup>, Diana Toneva<sup>1</sup>, Ivan Georgiev<sup>2,3</sup>, Stanislav Harizanov<sup>2,3</sup>, Dora Zlatareva<sup>4</sup>, Vassil Hadjidekov<sup>4</sup> and Nikolai Lazarov<sup>5,6</sup>

<sup>1</sup> Bulgarian Academy of Sciences, Institute of Experimental Morphology, Pathology and Anthropology with Museum, Department of Anthropology and Anatomy, Sofia, Bulgaria

<sup>2</sup> Bulgarian Academy of Sciences, Institute of Information and Communication Technologies, Department of Scientific Computations, Sofia, Bulgaria

<sup>3</sup> Bulgarian Academy of Sciences, Institute of Mathematics and Informatics, Department of Mathematical Modeling and Numerical Analysis, Sofia, Bulgaria

<sup>4</sup> Medical University of Sofia, Department of Diagnostic Imaging, Sofia, Bulgaria

<sup>5</sup> Medical University of Sofia, Department of Anatomy and Histology, Sofia, Bulgaria

<sup>6</sup> Bulgarian Academy of Sciences, Institute of Neurobiology, Department of Synaptic Signaling and Communications, Sofia, Bulgaria

## ABSTRACT

*Obliteration of the cranial sutures is an age-dependent process. Its premature occurrence (craniosynostosis) causes different craniofacial deformations, dependent on the affected suture(s). The understanding of the suture morphology and the remodeling processes during the obliteration is essential for early diagnosis and treatment of the premature closure. This study aimed to investigate the morphology of open and obliterated sutures and to perform comparison analysis on the 3D images obtained by both industrial and chemical computed tomography (CT) systems with various resolutions. A segment of the sagittal suture of dry skulls of known age and sex was scanned using Nikon XTH 225, an industrial CT system, developed by Nikon Metrology. The same section of the sagittal suture was observed on patients undergoing CT scanning with a multislice system Toshiba Aquilion 64 with 0.5 mm slice thickness. For 3D visualization, VGStudioMax 2.2 software was used. The suture morphology was observed in coronal section on sequential 2D slices. Micro-CT ( $\mu$ CT) scanning of dry skulls enabled calculation of the morphometric parameters and visualization of the microarchitecture of the suture and its reorganization during the obliteration, unlike the CT imaging of patients, where the sutures were scarcely discernable. In the entirely open sections of the suture the bone edges were separated by a gap of various widths. As the obliteration proceeded, the gap gradually reduced and the bone edges got into a contact. In the final stages, the traces from the contact faded away and the sutural area became a homogenous structure of increased integrity. The  $\mu$ CT scanning of dry bones is a powerful non-destructive technique for examination of the suture morphology. Remodeling of the suture during the obliteration leads to gradually diminishing of the gap between the bone edges to their entire coalescence.*

**Key words:** dry skull, suture microarchitecture, obliteration,  $\mu$ CT scanning, clinical CT imaging

## Introduction

Morphogenesis of the calvarian bones and facial complex is a lengthy developmental process initiated during early embryogenesis and completed during adulthood<sup>1</sup>. The calvaria is made up flat, intramembranous in origin bones, joined by sutures. During the fetal and early postnatal development the bones are unilaminar until the diploë appears and forms a trilaminar structure<sup>2</sup>. In adults, the calvarial bones consist of internal and external tables or layers of compact bone separated by a

vascular spongy bone space called diploë<sup>3</sup>. In humans, the end point of cranial vault growth is determined upon fusion of associated bones at about the third decade of life<sup>1</sup>.

The calvarial sutures (synarthrosis) are bands of fibrous connective tissue that fastened together apposed bones of the skull. The term »suture« is restricted to the connective tissues, whereas the term »sutural area« includes the adjacent edges of two opposing bones, together with the intervening soft tissues<sup>4</sup>. The conceptions of the sutures emphasize their open, functional status, not their eventual closure. Functioning sutures are the sites of

continuous bone deposition and resorption<sup>5</sup>. The sutures allow no active motions, but act as flexible joints and allow adjustive overlap of the calvarial bones as the head becomes compressed during the childbirth<sup>1,2,6</sup>. The resultant molding normalizes during the first week of life by cranial reexpansion and widening of the sutural areas<sup>5</sup>. As cranial sutures develop further during infancy, cranial adjustment to the expanding brain takes place by bone deposition at the sutural margins. To function as intramembranous bone growth sites, sutures need to remain patent, while allowing rapid bone formation at the edges of the bone fronts<sup>5</sup>.

Cranial suture sites have been thought to be determined by dural reflections<sup>5</sup>. The sutures developed initially by a wedge-shaped proliferation of cells at the periphery of the extending bone fields, termed »osteogenic fronts«, which appear to govern morphogenetic determination of sutural architecture. Osteogenic fronts could approximate each other by overlapping, leading to formation of an overlapping suture (e.g. the coronal suture), or in the same plane, which leads to development of an end-to-end type of suture usually observed in the midline and typical for the SS<sup>5</sup>. Both types of sutures could be modified during growth by secondarily developed interdigitations<sup>4</sup> dependent on different stress factors and suture maturation. The further bone growth at the sutural margins is secondary and passive in response to external separating forces<sup>5</sup>.

Normally, after the brain reach its optimal shape and size during early adulthood, the process of fusion of the adjacent calvarial bones, termed »obliteration«, slowly begins with a series of consequent morphological changes. These changes involve the sutural area and lead to complete covering up the traces of the contact between the adjacent cranial bones<sup>7</sup>. The underlying causes of both normal suture fusion in adulthood and premature fusion in craniosynostosis remain unclear<sup>6</sup>.

The premature closure of one or more sutures by fusion of bone fronts across the suture site prevents further bone formation at this site, and typically results in craniofacial dysmorphology<sup>1</sup>. This condition affects and distorts the configuration of the cranium and disturbs the growth and development of the brain<sup>1</sup>. The delayed closure or incomplete ossification of sutures and fontanelles is an opposite process, and there are several possible underlying mechanisms including a primary defect in the ossification, increased intracranial pressure, and direct infiltration of sutures by pathological tissue<sup>8</sup>. When patent sutures are widened because of hypoplastic bones or because of longstanding tension applied to patent sutures, wormian bones may develop<sup>5</sup>.

The study of craniosynostosis remains important because it provides a model for the study of suture fusion and the factors maintaining normal suture patency and function<sup>6</sup>. Numerous investigations have been carried out to establish if the normal suture closure is a regular part of the aging process and to define the sequence and the terms of suture obliteration regarding the age, but the results are controversial. Basically, the period of suture obliteration ranges from 2 years (e.g. metopic suture) to 70 years, when the cranial sutures are fully ossified<sup>9</sup>.

Clinical computed tomography (CT) scans from diagnostic imaging of patients have been used for investigation of the suture biology<sup>7,10</sup>, as well as scanning of dry skulls<sup>11</sup>. However, the micro-computed tomography ( $\mu$ CT) is a superior non-destructive highly accurate tool for the quantitative evaluation of calcified tissues<sup>12</sup> and provides three-dimensional reconstruction and morphometric analysis of bone at the trabecular level<sup>13</sup>. The  $\mu$ CT has enabled measurements from image datasets, representing the three-dimensional structure of trabecular bone. Thus, dependent on the specimens it could be obtained resolution between 10 and 75  $\mu\text{m}$ <sup>13</sup>, which enables the thinnest trabecular elements (70 microns in diameter) to be resolved<sup>14</sup>. All structural indices commonly determined from two-dimensional histologic sections can be obtained nondestructively from a large number of slices in each of three orthogonal directions. This permits a comprehensive description of structural variation within a specimen and greatly facilitates the study of structural anisotropy<sup>12</sup>.

Although previous researches considered the microarchitecture of an entirely open suture and craniosynostosis<sup>6,15,16</sup>, investigations on the normally obliterated sutures are scarce, especially on dry skulls. The sagittal suture (SS) has been accepted as the spot for initial commencement of the normal obliteration moreover, it was most commonly an initial site of craniosynostosis. Thus, the study aimed to compare the microstructure of open, fusing and already obliterated SS and to perform a quantitative stereological analysis of the suture segments and neighboring parietal bone fragments. Furthermore, we performed a comparison on the 3D images obtained by both industrial and clinical CT systems and discussed the opportunity of both technologies for cranial suture examination.

## Material and Methods

A selected segment of the SS along with the surrounding parietal bones was scanned in preserved dry skulls of adult males. The skulls belonged to soldiers died in the wars at the beginning of the 20th century: the First and the Second Balkan War and the First World War. Their bone remains were preserved in the Military Mausoleum with Ossuary, at the National Museum of Military History (Bulgaria) and data about the age at death was kept as an archive to the Museum. The sample includes 4 skulls aged between 34–47 years (M1-34; M2-43; M3-46; M4-47). The same SS section was observed on patients undergoing CT scanning with a multislice system Toshiba Aquilion 64 with 0.5 mm slice thickness aged between 20–80 years (M1-20; M2-34; M3-44; M4-80).

The  $\mu$ CT scanning was performed using Nikon XTH 225, an industrial CT system, developed by Nikon Metrology. The scanning parameters were: exposure time of 708 ms, voltage 90 kV, tube current 104  $\mu\text{A}$ . A total of 5000 projections were acquired as the object was rotated on 360° by steps of 0.072°. Region-of-interest CT scanning technique was applied in order to increase the spatial resolution of the reconstructed volume.

The reconstructions were performed using CT Pro 3D and .vgl files were generated. For 3D visualization of the bone segment representations and examination of the sequential slices VGStudioMax2.2. was used. The selection of ROIs, segmentation and morphometric calculations were performed using the same software. Visualization of the DICOM series from the clinical CT was inspected using VGStudioMax2.2 as well.

After reconstruction and visualization a volumetric rectangular region of interest (ROI) was selected restricted by the interdigitation of the suture line, as well as a commensurable part of the parietal bone next to the suture. Then the ROIs were extracted and segmentation algorithms were applied. Two phase segmentation involves binarizing an image such that only voxels above a certain linear attenuation value called threshold are considered foreground (bone), while the remaining ones are set as background (air). The threshold value was automatically determined, based on the gray-scale intensity histogram of the image. Calculation of the main morphometric parameters was performed on the segmented ROIs, including the trabecular bone and the cortical layers:

- Bone volume fraction (BV/TV), the percentage of the ROI occupied by bone;
- Ratio of bone surface to bone volume (BS/BV) is the internal surface area of a bone sample compared with its total volume;
- Trabecular thickness (Tb.Th), the diameter of the largest sphere which is entirely bounded within the solid surfaces;
- Trabecular number (Tb.N), the number of traversals across a trabecular or solid structure made per unit length on a random linear path through the ROI;
- Trabecular separation (Tb.Sp), the thickness of the spaces as defined by binarization within the ROI, interpreted as the thickness of the marrow cavities;
- Degree of anisotropy (DA) is a measure of 3D symmetry or the presence or absence of preferential alignment of structures along a particular directional axis and can assume values in the range 0 (isotropic) to 1 (anisotropic).

## Results

### Clinical CT imaging:

Since the thinnest trabecular elements have a diameter of  $70 \mu\text{m}^4$ , the obtained resolution of 0,5 mm from the CT-scanning of patients was too low. The obtained imaging allowed only gross 2D cross-sectional inspection of the contact between the adjacent bones without any details (Figure 1). Thus, although the large datasets were generated from CT scans of patient, the low resolution disabled an adequate cranial suture examination and morphometric parameters evaluation.

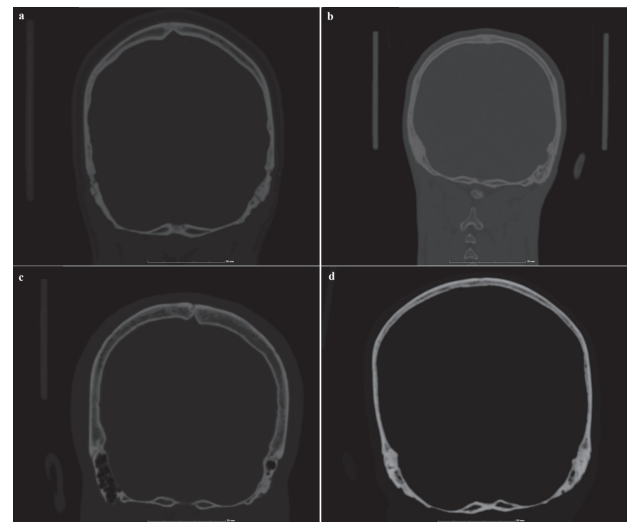


**Fig. 1.** Imaging obtained by clinical CT. Coronal sections at the level of the sagittal suture: a) in a 20 year old male; b) in a 34 year old male, c) in a 44 year old male; d) in a 80 year old male.

### $\mu\text{CT}$ imaging:

Morphometrics, quantifiable bone architecture and morphology

The calculated stereological parameters for the suture segments are presented in Table 1. The same parameters

**TABLE 1**  
MORPHOMETRIC PARAMETERS OF THE SAGITTAL SUTURE FRAGMENTS

Stereologic parameters	M34	M43	M46	M47
BV/TV (%)	0.387454	0.413645	0.377307	0.520325
BS/BV (mm <sup>2</sup> /mm <sup>3</sup> )	2.75396	1.64826	1.44885	2.32826
Tb.Th (mm)	0.726228	1.2134	1.3804	0.859012
Tb.N (1/mm)	0.533515	0.340898	0.273331	0.605725
Tb.Sp (mm)	1.14813	1.72003	2.27817	2.29983
Anisotropy	0.272262	0.37515	0.329746	0.326592
Dimension in mm	14.6x13.9x34.9	9.8x10.2x34.5	10.9x12.9x35.6	8.5x11.6x31.6
Resolution ( $\mu\text{m}^3$ )	24.65418	24.272	24.86621	22.42661

**TABLE 2**  
MORPHOMETRIC PARAMETERS OF THE BONE FRAGMENTS NEXT TO THE SAGITTAL SUTURE

Stereologic parameters	M34	M43	M46	M47
BV/TV (%)	0.373068	0.313401	0.284761	0.254019
BS/BV (mm <sup>2</sup> /mm <sup>3</sup> )	2.72236	2.08585	1.84713	2.43816
Tb.Th (mm)	0.734656	0.958841	1.08276	0.82029
Tb.N (1/mm)	0.507814	0.326854	0.262996	0.30967
Tb.Sp (mm)	1.23457	2.10063	2.71958	2.40895
Anisotropy	0.262911	0.380536	0.364287	0.359028
Dimension (x:y:z) in mm	18.4x12.0x35.2	10.9x11.2x34.7	14.3x16.3x34.7	10.4x13.3x31.5
Resolution (μm <sup>3</sup> )	24.65418	24.272	24.86621	22.42661

computed for the parietal bone segments neighboring the suture pieces are presented in Table 2)

Cross-sectional observation on sequential 2D slices:

In the open segments of the SS, a wide gap between the adjacent bone edges could be seen (Figures 2 and 3a). The suture line was interdigitated and the bone margins were distinguishably compact (Figure 3a). In the fragments with advanced stage of closure or already obliterated SS suture, the margins of the adjacent bones came into a tight contact one with another (Figures 4 and 5) as in some loci gaps of different width could be seen (Figures 5b and 5c) on either of the tree layers (internal, external lamina, diploë). With advances of the obliteration the suture areas became more homogenous and resembled by structure the surrounding bone (Figures 5a and 5b). However, the suture line could be clearly traced following the discernable denser area, where both margins were in a contact and got fused (Figures 3 and 6).

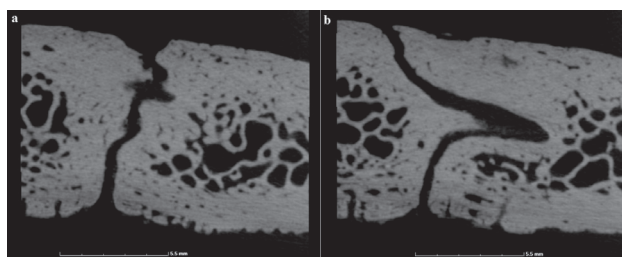


**Fig. 2** μCT imaging of an open sagittal suture in a dry skull of 34 year old male. Coronal section through the suture. A wide gap between the adjacent bone edges could be seen.

**Discussion**

The cause of suture closure is still unclear. Suture closure has been attributed to vascular, hormonal, genetic, mechanical, and local factors<sup>5</sup>. The actual mechanisms that result in pathologic synostosis are heterogeneous in nature and are not in all cases a normal suture closure commencing too early. However, in craniosynostosis the proper suture formation occurs, but physiologic completion is accelerated<sup>5</sup>.

Through a diagnostic imaging of patients a large datasets of clinical CT scans were generated. However, the low resolution was the main shortcoming which impeded the

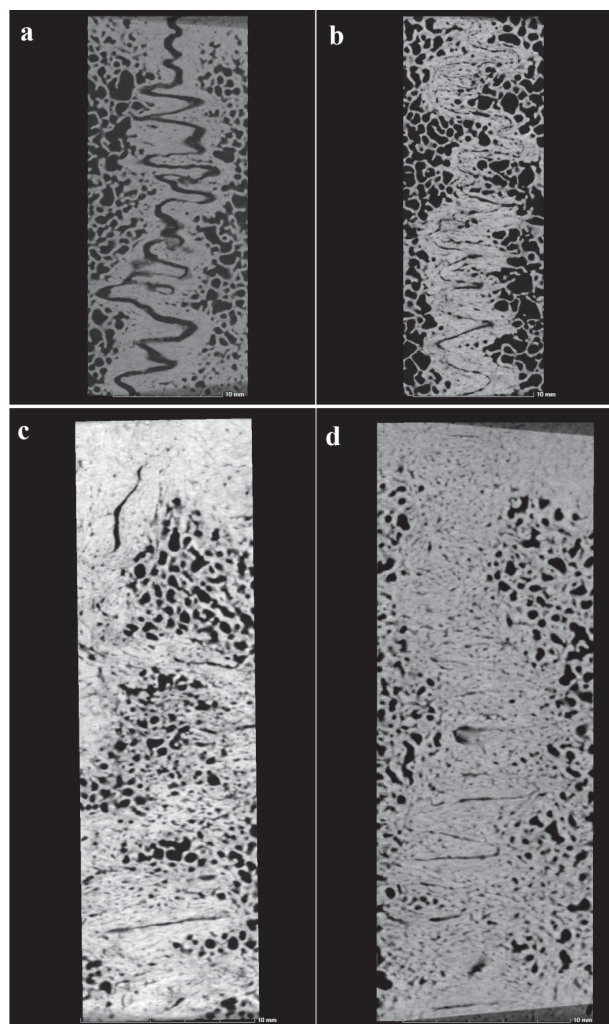


**Fig. 3.** μCT imaging of an open sagittal suture, and different stages of obliteration in transversal section at the level of the diploë. Sagittal suture: a) in a 34 year old male; b) in a 47 year old male; c) in a 43 year old male; d) in a 46 year old male.

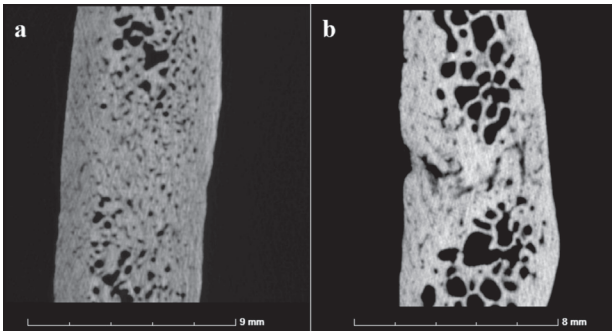


**Fig. 4.**  $\mu$ CT imaging of the sagittal suture in coronal section: a) in a 46 year old male; b) in a 47 year old male.

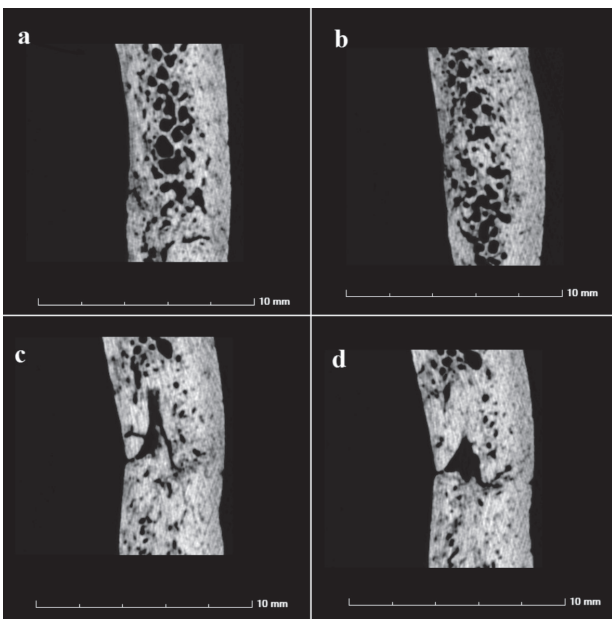


**Fig. 5.**  $\mu$ CT imaging of the sagittal suture in a 43 year old male, coronal sections: a-b) a homogeneous internal structure; b-c) a gap between the bone edges.

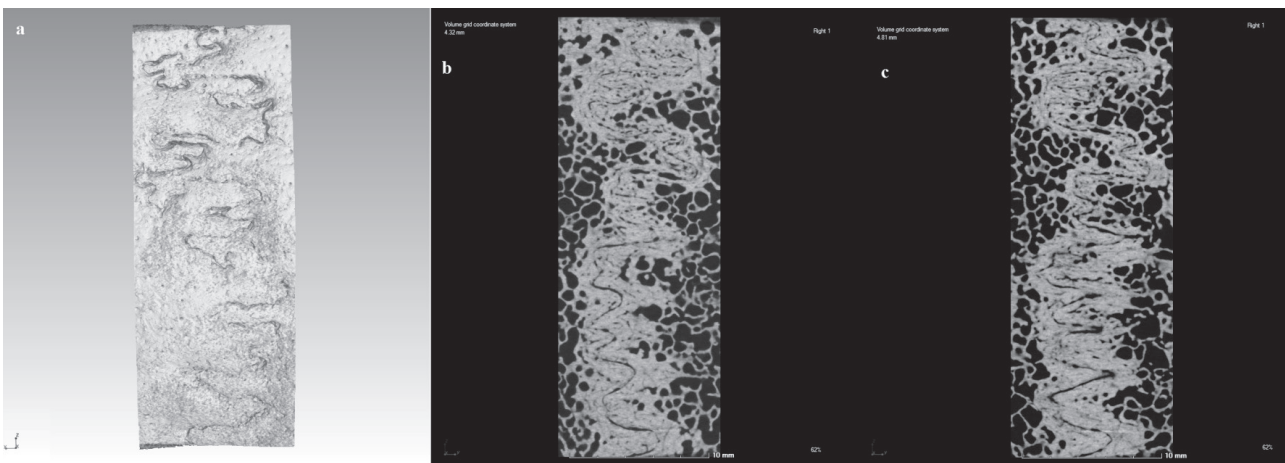


**Fig. 6.**  $\mu$ CT imaging of the sagittal suture in a 47 year old male: a) 3D representation of the bone fragment; b-c) transversal sections at the level of the diploë.

examination of the suture morphology and calculation of the morphometric parameters on this database. The resolution in  $\mu$ CT scanning was inversely proportional to the specimen size<sup>6</sup> (Anderson et al., 2006). Thus, dependent of the specimens' size, the used  $\mu$ CT system allowed obtaining a resolution from 3  $\mu$ m up to 98  $\mu$ m. The resolution for the specimens in this study ranged between 22.4 – 24.9  $\mu$ m, and was suitable for differentiation of the thinnest trabeculae and reliable morphometric analyses.

Morphometrics, quantifiably bone architecture and morphology:

Cancellous bone has a porous microstructure with numerous small interconnected trabeculae (100–300  $\mu$ m of thickness, 300–1500  $\mu$ m spacing between adjacent trabeculae) and a high surface area<sup>17</sup>.  $\mu$ CT has the advantage to measure directly the bone microarchitecture without relying on stereologic models as is done with standard histologic evaluations<sup>18</sup>.

Similarly to the results obtained by Sherick et al.<sup>13</sup> from a comparison of open and prematurely synostosed sutures, the comparison of the morphometric parameters among our SS fragments showed that the obliterated specimens contained more bone and less surface area than the non-obliterated one. The trabeculae of the obliterated fragments were thicker, had a relatively higher density, and were spaced farther apart than in the open suture. The anisotropy as a quantitative measure of trabecular polarization showed that the obliterated fragments were with »less orderedness« compared to the open one.

The comparison of the fragment containing an open SS with the fragment from the parietal bone next to the suture showed less differences compared to the analogous juxtaposition for the obliterated fragments, as the differences were greatest in the oldest individual (Tables 1 and 2). The comparison of bone architecture of the non-suture fragments i.e. as the age advanced showed a diminishing of the bone fraction (BV/TV), the internal surface area (BS/BV) and the trabeculae number (Tb.N), as well as an increase of the trabeculae thickness (Tb.Th), the marrow

spaces (Tb.Sp) and the degree of anisotropy (DA) (Table 2). The structural anisotropy in cancellous bone is evident from simple inspection, but a numerical estimate of the degree of anisotropy is crucial for understanding the biomechanical properties of normal suture morphology<sup>12</sup>. In our samples, it could be seen that the anisotropy increased with the suture obliteration (Table 1) and age advance (Table 2).

Morphological changes and suture remodeling during closure:

The open suture was characterized by a wide gap between the compact bone margins, and could be easily recognized on clinical CT imaging (Figure 1). However, the degree of fusion in the stages of progressive suture obliteration was difficult for demarcation on those imaging. The  $\mu$ CT provided a clear visualization of the contact between the adjacent bone margins as well as the quantitative assessment of the degree of bone mineralization and parasutural sclerosis. Thus, the imaging techniques and resolution should be carefully taken into account when comparing data about the suture morphology.

It has been established that in the process of maturation the suture undergoes variable morphological changes related to a reorganisation of the bone microarchitecture, which finally lead to its ossification. According to Skrzat et al.<sup>11</sup>, when the obliteration proceeds the sutural gap ceases and the laminae and diploic layers of the two adjacent bones become a single structure of increased integrity, and these changes are often accompanied by a degeneration of the inner compact bone layer. Anderson et al.<sup>6</sup> have asserted that with the normal maturation the suture microarchitecture becomes similar to the pattern of the adjacent bone, but relatively denser. Furthermore, Furuya et al.<sup>7</sup> have observed that with the age advance the apposition of the sutures becomes closer and parasutural sclerosis develops. If the suture line is visible, the parasutural mineralization could be identified, but when the suture is absent, either a single linear area of bone mineralization could be seen, or there are no traces from the suture at all<sup>7</sup>. Our observation confirmed the previous findings, but without the degeneration of the inner compact bone layer. These changes could be marked on the imaging obtained by clinical CT (Figure 1). The  $\mu$ CT imaging, however, clearly visualized the area of the increased bone density

representing remnants of the bone margins following the suture interdigitation (Figures 3 and 6).

According to Anderson et al.<sup>6</sup>, the open sutures demonstrate marked interdigitation of the adjacent bone margins in the normal open suture, and where the suture remains open but will close shortly the bone margins are rounded with no interdigitation. What we observed was that the degree of the interdigitation was not related with the stage of the obliteration.

In initial sutural obliteration, slender bone spicules extended from the sutural margins, bridging the sutural gap either partially or completely<sup>5</sup>. Initial fusion in the SS can take place anywhere along its entire length, and there is no predilection to begin at any one point. Fusion may begin on either the endocranial or ectocranial surface, although it occurs more commonly in the former<sup>5</sup>. Later, the bone microarchitecture matures along the suture and rapidly becomes undistinguishable from the pattern in the adjacent bone<sup>6</sup>. However, gaps of different widths could be seen on either of the calvarial bone layers in the obliterated suture (Figure 5).

## Conclusion

Understanding of the normal suture biology and maturation will contribute to knowledge and prevention of the craniosynostosis. The dry skulls from individuals of known age and sex are suitable objects for qualitative and quantitative studying of the cranial suture morphology i.e. the contact between the bone margins of the adjacent bones using  $\mu$ CT imaging. Furthermore, the 3D imaging of dry bones is beneficial for segmentation due to the fact that the images are composed of two-phases i.e. bone and air without other components.

## Acknowledgments

This study was supported by the National Science Fund of Bulgaria, grant DN01/15-20.12.2016

The authors would like to acknowledge the kind assistance given by the staff of the National Museum of Military History (Bulgaria).

## REFERENCES

- OPPERMAN LA, *Dev Dyn*, 219(4) (2000), 472. DOI: 10.1002/1097-0177 (2000)9999:9999<:AID-DVDY1073>3.0.CO;2-F. — 2. TUBBS RS, BOSMIA AN, COHEN-GADOL AA, *Child's Nervous System*, 28 (2012), 23. DOI: 10.1007/s00381-011-1637-0. — 3. SKRZAT J, BRZEGOWY P, WALOCHA J, WOJCIECHOWSKI W, *Folia Morphol (Warsz)*, 63(1) (2004), 67. — 4. MOSS ML, *Anat Rec*, 127(3) (1957) 569. DOI: 10.1002/ar.1091270307. — 5. COHEN MM JR, *Am J Med Genet*, 47(5) (1993), 581. DOI: 10.1097/01.scs.0000230019.46896.b0. — 6. ANDERSON PJ, NETHERWAY DJ, DAVID DJ, SELF P, *J Craniofac Surg*, 17(5) (2006), 909. DOI: 10.1097/01.scs.0000230019.46896.b0. — 7. FURUYA Y, EDWARDS MS, ALPERS CE, TRESS BM, OUSTERHOUT DK, NORMAND, *J Neurosurg*, 61(1) (1984), 53. DOI: 10.3171/jns.1984.61.1.0053. — 8. CAST-RIOTA-SCANDERBEG A, DALLAPICCOLA B, *Abnormal skeletal phenotypes* (Springer Verlag, Berlin Heidelberg, 2005). — 9. TODD TW, LYON DW, *Am J Phys Anthropol*, 8(1) (1925), 23. DOI: 10.1002/ajpa.1330080103. — 10. CHIBA F, MAKINO Y, MOTOMURA A, INOKUCHI G, TORIMITSU S, ISHII N, SAKUMAA, NAGASAWA S, SAITOH H, YAJIMA D, HAYAKAWA M, ODO Y, SUZUKI Y, IWASE H, *Int J Legal Med*, 127(5) (2013), 1005. DOI: 10.1007/s00414-013-0883-y. — 11. SKRZAT J, BRZEGOWY P, WALOCHA J, *Folia Morphol (Warsz)*, 61(4) 2002, 257. — 12. FELDKAMP LA, GOLDSTEIN SA, PARFITT AM, JESION G, KLEEREKOPER M, *J Bone Miner Res*, 4(1) (1989), 3. DOI: 10.1002/jbmr.5650040103. — 13. SHERICK DG, BUCHMAN SR, GOULET RW, GOLDSTEIN SA, *Cleft Palate Craniofac J*, 37(1) (2000), 5. DOI: 10.1597/

1545-1569(2000)037<0005:ANTFTQ>2.3.CO;2. — 14. PARKINSON IH, FAZZALARI NL, Characterisation of Trabecular Bone Structure. Skeletal Aging and Osteoporosis. In: Studies in Mechanobiology, Tissue Engineering and Biomaterials, (Springer, vol. 5, 2012), 31. DOI: 10.1007/8415\_2011\_113 — 15. OZAKI W, BUCHMAN SR, MURASZKO KM, COLEMAN D, Plastic and Reconstr Surg, 102 (1988), 1385. — 16. COREGA C, VAIDA L, BĂCIUȚ M, SERBĂNESCU A, PALAGHIȚĂ-BA-

NIAS L, Rom J Morphol Embryol, 51(1) (2010), 123. — 17. SILVA AMH, ALVES JM, DA SILVA OL, FERREIRA NJ, GAZZIRO M, PEREIRA JC, LASSO PRO, VAZ CMP, PEREIRA CAM, LEIVA TP, GUARNIERO R, Journal of Physics. Conference Series (Online), 313 (2011), 1. DOI: 10.1088/17-42-6596/313/1/012008 — 18. BOUXSEIN ML, BOYD SK, CHRISTIANSEN BA, GULDBERG RE, JEPSEN KJ, MÜLLER R, J Bone Miner Res, 25(7) (2010), 1468. DOI: 10.1002/jbmr.141

S. Nikolova

*Bulgarian Academy of Sciences, Institute of Experimental Morphology, Pathology and Anthropology with Museum, Department of Anthropology and Anatomy Acad. G. Bonchev Str., Bl. 25, BG-1113 Sofia, Bulgaria*  
E-mail: sil\_nikolova@abv.bg (S. Nikolova)

## **CT-STUDIJA MORFOLOGIJE KRANIJALNIH ŠAVOVA I NJEZINE REORGANIZACIJE TIJEKOM OBLITERACIJE**

### **SAŽETAK**

Obliteriranje kranijalnih šavova je proces koji ovisi o dobi. Njegova prerana pojava (kraniosynostosis) uzrokuje različite kraniofacijalne deformacije, ovisno o zahvaćenom šavovima (s). Razumijevanje morfologije šavova i procesa remodeliranja tijekom uklanjanja ključno je za ranu dijagnozu i liječenje preranog zatvaranja. Ova je studija usmjerena na istraživanje morfologije otvorenih i zanemarenih šavova te za analizu usporedbe na 3D snimkama koje su dobivene industrijskim i medicinskim kompjutoriziranim tomografskim (CT) sustavima s različitim rezolucijama. Segment sagitalnih šavova suhih lubanja poznatog doba i spola skeniran je pomoću Nikon XTH 225, industrijskog CT sustava, kojeg je razvio Nikon Metrology. Ista sekcija sagitalnih šavova promatrana je kod bolesnika koji su podvrgnuti CT skeniranju s višestrukim sustavom Toshiba Aquilion 64 s debljinom od 0,5 mm. Za 3D vizualizaciju korišteni su VGStudioMax 2.2. Morfologija šavova uočena je u koronalnom dijelu na sekvencijalnim 2D rezovima. Mikro CT ( $\mu$ CT) skeniranje suhih lubanja omogućilo je izračunavanje morfometrijskih parametara i vizualizaciju mikroarhitekture šavova i njegovu reorganizaciju tijekom obliteracije, za razliku od CT snimanja pacijenata, gdje su šavovi jedva prepoznatljivi. U potpuno otvorenim dijelovima šavova rubovi kostiju bili su odvojeni jazom različitih širina. Kako je nastajalo uništavanje, razmak se postupno smanjivao i rubovi kostiju stupili su u kontakt. U posljednjim fazama tragovi iz kontakta izbljedjeli i sutralno područje postalo je homogena struktura povećane integriteta. MCT skeniranje suhih kostiju moćna je nerazorna tehnika za ispitivanje morfologije šavova. Pregradnja šavova za vrijeme uklanjanja dovodi do postupno smanjenja jaza između rubova kosti do njihove cjelovite koalescencije.